NASA TECHNICAL NOTE

N73-32554

NASA TN D-7423

NASA TN D-7423

EFFECTS OF NUCLEAR RADIATION ON A HIGH-RELIABILITY SILICON POWER DIODE

IV - Analysis of Reverse Bias Characteristics

by Julian F. Been

Lewis Research Center

Cleveland, Ohio 44135

NATIONAL AERONAUTICS AND SPACE ADMINISTRATION • WASHINGTON, D. C. • OCTOBER 1973

1. Report No.	2. Government Accession No.	3. Recipient's Catalog No.
NASA TN D-7423		

4. Title and Subtitle	5. Report Date
EFFECTS OF NUCLEAR RADIATION ON A HIGH-RELIABILITY SILICON POWER DIODE IV - ANALYSIS OF REVERSE BIAS CHARACTERISTICS	October 1973
	6. Performing Organization Code

7. Author(s)	8. Performing Organization Report No.
Julian F. Been	E-7362
	10. Work Unit No. 502-25

9. Performing Organization Name and Address	11. Contract or Grant No.
Lewis Research Center National Aeronautics and Space Administration Cleveland, Ohio 44135	

12. Sponsoring Agency Name and Address	13. Type of Report and Period Covered
National Aeronautics and Space Administration Washington, D.C. 20546	Technical Note
	14. Sponsoring Agency Code

15. Supplementary Notes

16. Abstract

The effects of nuclear radiation on the reverse bias electrical characteristics of one hundred silicon power diodes were investigated. It was found that on a percentage basis the changes in reverse currents were large but, due to very low initial values, this electrical characteristic would not be the limiting factor in use of these diodes. These changes were interpreted in terms of decreasing minority carrier lifetimes as related to generation-recombination currents. The magnitudes of reverse voltage breakdown were in most instances unaffected by irradiation.

17. Key Words (Suggested by Author(s))	18. Distribution Statement
Radiation effects Nuclear radiation Silicon diodes Electrical characteristics	Unclassified - unlimited

19. Security Classif. (of this report)	20. Security Classif. (of this page)	21. No. of Pages	22. Price*
Unclassified	Unclassified	34	Domestic, $3.00 Foreign, $5.50

* For sale by the National Technical Information Service, Springfield, Virginia 22151

EFFECTS OF NUCLEAR RADIATION ON A HIGH-RELIABILITY SILICON POWER DIODE

IV - ANALYSIS OF REVERSE BIAS CHARACTERISTICS

by Julian F. Been

Lewis Research Center

SUMMARY

The effects of nuclear radiation on the reverse bias electrical characteristics of one hundred, 35-ampere, 600-volt peak inverse, high-reliability silicon power diodes were investigated. The diodes were irradiated in the NASA Plum Brook Nuclear Reactor for a total time of approximately 480 hours. The resultant fast neutron (0.1 MeV and above) fluence was 5×10^{13} neutrons per square centimeter and a gamma dose of 3×10^{7} rads (C). Diodes before irradiation had very low reverse currents, sharp breakdown knees but considerable spread in voltage at a given current among the diodes. Some diode curves showed irregularities in that as the voltage was increased the current increased in an uneven manner. This generally occurred in the higher voltages (100 V and up). The effect of radiation was to increase the reverse currents for given voltages up to approximately 100 volts. Above this value, approximately 30 percent showed decreases in reverse currents with radiation. These decreases were generally associated with the irregular shaped curves in that irradiation tended to minimize the irregular shapes. Irradiating the diodes at different temperatures and in different operating modes made no notable difference in the reverse characteristics. The reverse voltage breakdown knee remained identifiable although the knee became more rounded. The magnitude of avalanche voltage in general remained relatively constant.

A theoretical curve for preirradiated diodes was calculated, and compared to experimental results. An estimate was made of the effects or radiation at the lower voltages where fair agreement was obtained. At higher voltages (above 100 V) the effects of radiation were unpredictable due to the irregular curves. An attempt was made with little success to correlate the irregularly shaped curves, (and associated effects of irradiation on them), with other changes in electrical characteristics such as change in capacitance and forward voltage drop.

The results of this test allow a diode to be made more radiation tolerant by utilizing the trade-offs in the very low reverse currents and high breakdown voltages for improved forward electrical characteristics.

INTRODUCTION

Whenever semiconductors are used as part of a nuclear electric power generating system, it is generally accepted that the semiconductors are the most sensitive components to nuclear radiation in that system. In space power applications where it may not be possible to locate or shield components to obtain radiation of acceptable levels, testing becomes necessary to determine how much those semiconductors, contemplated for system use, will tolerate before failure. Generally it is desirable to know more than the fact that a device failed to perform its intended function in a circuit. If it can be determined how each electrical characteristic changed, steps can be taken to improve a particular characteristic. This can be accomplished through correlating the basic parameters of the device to its electrical characteristics and altering those parameters in such a way as to improve that particular electrical characteristic with respect to radiation damage. Changes in the basic parameters or geometry of the device to accommodate one electrical characteristic to radiation effects generally means a trade-off in another electrical characteristic. It is therefore necessary to investigate several of the important electrical characteristics and the effects of radiation on them to determine the most feasible way to improve radiation tolerance.

The discussion and analysis in this report pertains to the reverse biased electrical characteristics, that is, the reverse currents and breakdown voltages and the effects of nuclear radiation on them. Considerable work has been done by investigators in the area of reverse biased junctions (refs. 1 and 2) and the effects of radiation on them (ref. 3). Like the forward electrical characteristics (ref. 4) the mechanisms governing the reverse current as a function of voltage depend upon the basic parameters and geometry of the silicon chip. Of the three components of the reverse current; diffusion, generation-recombination and surface, the first two have established relations between the basic device parameters including geometry of the device and the current components. The surface component is less defined and is therefore less predictable. This investigation attempted to compare calculated with experimental values of the reverse electrical characteristics of a 35-ampere, 600-volt peak inverse (PIV) silicon power diode and to examine the effects of radiation on them.

DESCRIPTION OF DIODES TESTED

The diode investigated was an S1N1189. The prefix "S" in the part number indicates that the diode passed the NASA Marshall Space Flight Center screening and performance specification (ref. 5). The silicon chip configuration is shown in figure 1 and has an n^+-p-p^+-type junction prepared by a double-diffusion process. The base region p-material is doped to 1.4×10^{14} to 2.0×10^{14} boron atoms per cubic centimeters (mini-

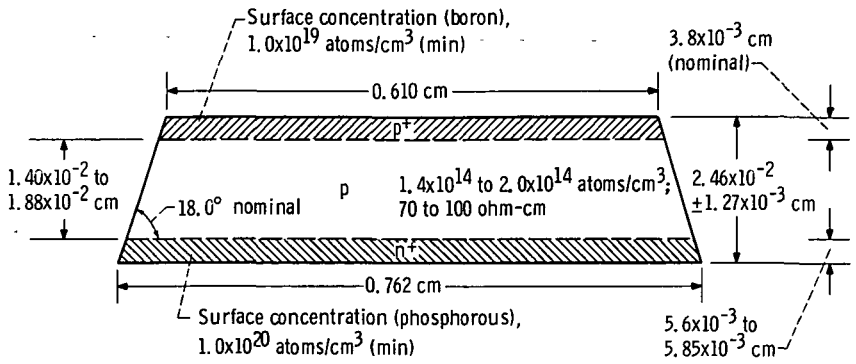

Figure 1. - Silicon chip configuration of S1N1189. (Drawing not to scale.)

mum). The nominal depth of the p-junction is 38 micrometers. The n-region has a surface dopant concentration of 1.0×10^{20} phosphorous atoms per cubic centimeter (minimum) with a nominal n-p junction depth of 57 micrometers. The chip is circular with sides beveled to a minimal 18^{o} slope, which lowers the electric field at the surface (ref. 6). The beveled sides are coated with a silicone rubber to form a passivation layer on the surface. The nominal diameter of the chip on the p-side is 0.61 centimeter and 0.76 centimeter on the n-side. The overall thickness of the chip is approximately 2.54×10^{-2} centimeter.

DESCRIPTION OF IRRADIATION

The two factors expected to be most important in modifying the damage due to nuclear radiation in an operating space power system are the operating temperature and current.

The irradiation testing of the diodes actually consisted of two separate tests. In each, 50 diodes were irradiated simultaneously in the reactor under similar conditions, with the important difference being the case temperature at which the two sets of diodes were irradiated. Each test set of 50 diodes was divided into groups according to the operating modes given in table I. (Symbols are defined in appendix A.) Operating currents and voltages were determined primarily by normal derating at the lower temperatures.

All diodes in each test were operated in the modes (table I) during irradiation except when measurements were taken. The irradiation of each test set proceeded for two reactor cycles, the nominal reactor cycle being 10 days at rated power, depending on the reactor power scheduling. The average temperatures of the diodes during irradiation (table I) were different for the three operating groups because one coolant line served all the diodes on each test plate, and each diode was its own heat source. For

TABLE I. - DIODE GROUPING FOR EACH TEST BY OPERATING MODES WITH AVERAGE INITIAL AND FINAL IRRADIATION TEMPERATURES

Group	Diodes per set	Operating mode	Set			
			I		II	
			Neutron fluence, neutrons/cm^2			
			4.6×10^{13}		4.0×10^{13}	
			Average temperature, T, ^{o}C			
			Initial	Final	Initial	Final
A	10	Forward current, 10 A dc	48.5	60	106	125
B	10	Reverse bias, 100 V dc	38	43	103	102
C	30	ac rectification; average forward current, 10 A; peak reverse voltage, 150 V	50.5	66	99	124
Nominal temperature			----	60	---	120

example, the reverse bias group generated less heat than the forward bias group and therefore operated at lower temperatures. Table I also includes the change in average operating temperatures as each test progressed. As used in this report, designated nominal temperatures represent the average final temperature.

The first set of diodes (test I, 60^{o} C nominal) received a fast-neutron ($\geq$0.1 MeV) fluence of $4.6\pm1.5\times10^{13}$ neutrons per square centimeter, and the second set of diodes (test II, 120^{o} C nominal) received $4.9\pm1.6\times10^{13}$ neutrons per square centimeter (ref. 7). The gamma dosage for each set of diodes was $3.2\pm0.6\times10^{7}$ rads (C).

The methods for determining the fast-neutron flux and gamma dosage and the conditions for which a calculated flux can be obtained are described in references 7 and 8.

DISCUSSION AND ANALYSIS

Current-Voltage Calculations

Low reverse bias (0.010 to 100 V) for unirradiated diodes. - The reverse current for a diode is made up of three components; generation-recombination, diffusion and surface components. This is similar to a forward bias diode at very low biases. As the voltage is increased, however, different components will dominate depending on whether it is reverse or forward bias. If enough information is known about the diode, the three components of current can be calculated and added together such that their sum should be comparable to the experimental data. Through additional temperature and capacitance measurements enough information was obtained to calculate the generation-recombination and the diffusion current components. Details of this analysis are in appendix B.

Figure 2 shows calculated and measured current for a single diode as a function of voltage from 1.0 millivolt to 100 volts. The generation-recombination and diffusion components are comparable in magnitude up to approximately 100 millivolts where the diffusion component becomes essentially constant. Above this voltage the generation-

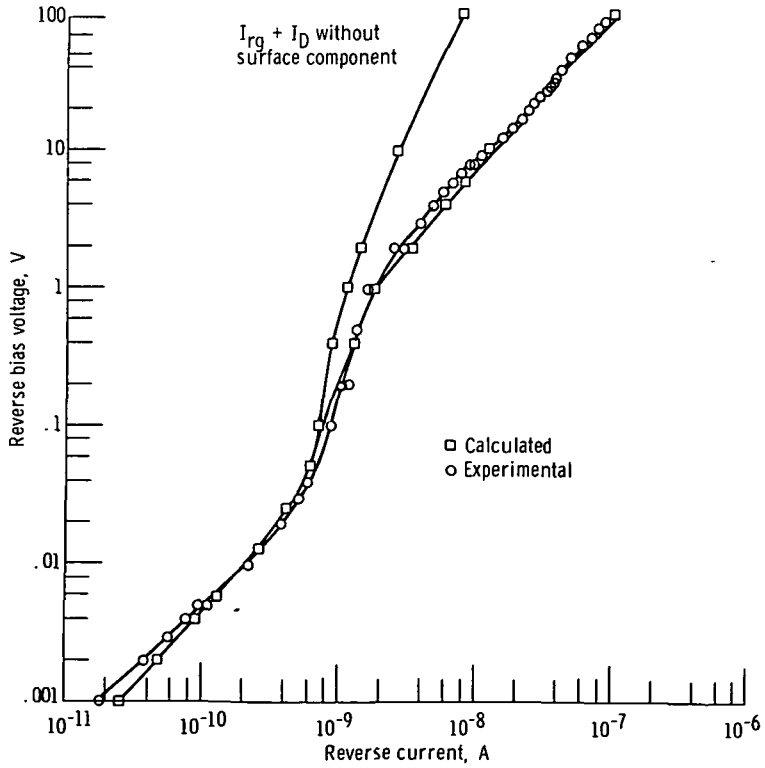

Figure 2. - Reverse current-voltage characteristics (range of 1.0 mV to 1000 V reverse bias) for diode 805 before irradiation.

recombination component becomes much larger than the diffusion component. The calculations for the generation-recombination current were based on the depletion region width increasing as the applied voltage to the one half power above an applied voltage of 1 volt. This was in agreement with capacitance-voltage measurements.

The magnitude of the calculated current components and the shape of the curves are comparable to the experimental results at very low voltages. At higher voltages, however, the added components of generation-recombination and diffusion are considerably smaller than the experimental values. It can be postulated that a large part of the difference in the calculated and the experimental values was due to a surface component since above approximately 1.0 volt the current was almost a linear function of voltage. This is the type of relation that would be expected from a resistive surface leakage.

When a resistive current component was calculated, based on an assumed 10^9 ohms surface resistance for this particular diode, there was good agreement with experimental values including the higher voltages up to 100 volts, as seen in figure 2. Even assuming a fair degree of uniformity in the fabrication process, it would not be expected that this surface resistance would be the same for each diode. The surface component of current therefore might be the least predictable of the three current components and therefore contribute to the large variation of total reverse currents observed among the diodes.

Effects of radiation damage at low reverse bias. - The direction of change in the reverse current due to irradiation at low reverse bias (100 V and below) is consistent and predictable. The magnitude of change, however, is not as consistent nor predictable due to the variation in data from individual diodes, and to the five orders of voltages and current considered, as figure 2. The fact that the minority carrier lifetime decreases due to radiation induced recombination centers has been established (refs. 3, 9 and 10). The amount of decrease is dependent upon a number of factors such as the energy of the incident radiation, type of radiation, amount of radiation, and so forth. Examination of equation (B1) would indicate that (1) generation-recombination component of current should increase and (2) it should increase inversely proportional to the decreasing minority carrier lifetime $\sqrt{\tau_{po}\tau_{no}}$. The change in the effective minority carrier lifetime was determined in appendix C by measuring the change in reverse current during irradiation on a sample group and calculating a damage constant K_s for silicon. The measurements were made at 100 volts reverse bias to minimize the effects, at lower voltages, of the diffusion component of current, and yet stay below those voltages where the current varied irregularly with increasing voltages. There was considerable variation in the damage constant K_s and therefore in the effective minority carrier lifetime τ_{eff}. The average change in τ_{eff} for the low temperature cycles was approximately a factor of ten; however, the τ_{eff} for individual diodes varied considerably more. This indicates that caution must be used when applying these sample calculations to individual diodes. However, applying these results to equation (B1); the generation-

recombination current should increase by some factor of approximately ten. The diffusion component (eq. (B2)), however, will be affected less, that is, through the relation $L = \sqrt{D\tau}$, so that the diffusion component will increase by the factor $\sqrt{\tau_{after}/\tau_{before}}$. When both components are considered at 100 volts, if the increase is due to the change in effective τ_{eff}, the total reverse current should increase by approximately a factor of ten. Comparing this change with the diode considered previously (fig. 3), there is reasonable agreement at this bias.

Below 100 volts bias the change in reverse current was generally greater than a factor of ten. Although no measurements were made to check the effects of radiation on the surface of the semiconductor chip, it is possible that ionization paths or channels formed which would alter the reverse electrical characteristics. Since these surface states can have different generation-recombination rates (ref. 2), it is possible that the greater changes than predicted were due to these surface effects.

The curve also straightens out with radiation such that it is a much smoother curve

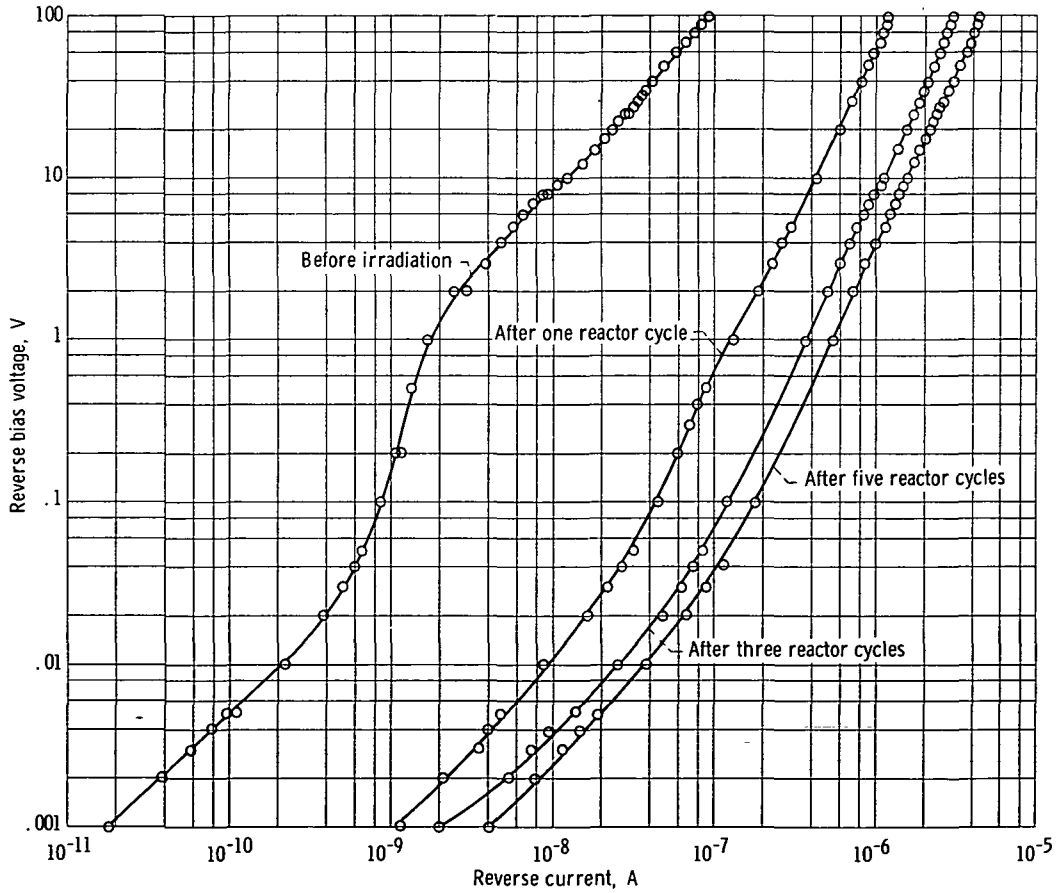

Figure 3. - Curves showing effects of radiation on reverse current-voltage characteristics (range of 1.0 mV to 1000 V reverse bias) for diode 805. (Neutron fluence for one reactor cycle is approximately 2.5×10^{13} neutrons/cm^2.)

and more closely follows a $V^{1/2}$ slope, as would be expected above approximately 1.0 volts bias. This smoothing is principally due to the fact that with the decreasing minority carrier lifetime, the diffusion component becomes a considerably smaller portion of the total reverse current at the lower voltages.

High reverse bias (above 100 V) for unirradiated diodes. - Some general statements can be made as to the current-voltage characteristics at higher voltages which are considered to be more nearly the operating voltages of the device: (1) all preirradiated reverse currents were very low (10^{-6} to 10^{-7} A) at the rated voltage of 600 volts; (2) all diodes had relatively sharp avalanche breakdown voltage; and (3) the reverse bias curves tend to group into two classes, normal and irregular. The curves which were considered normal were those whose currents increased smoothly as the reverse

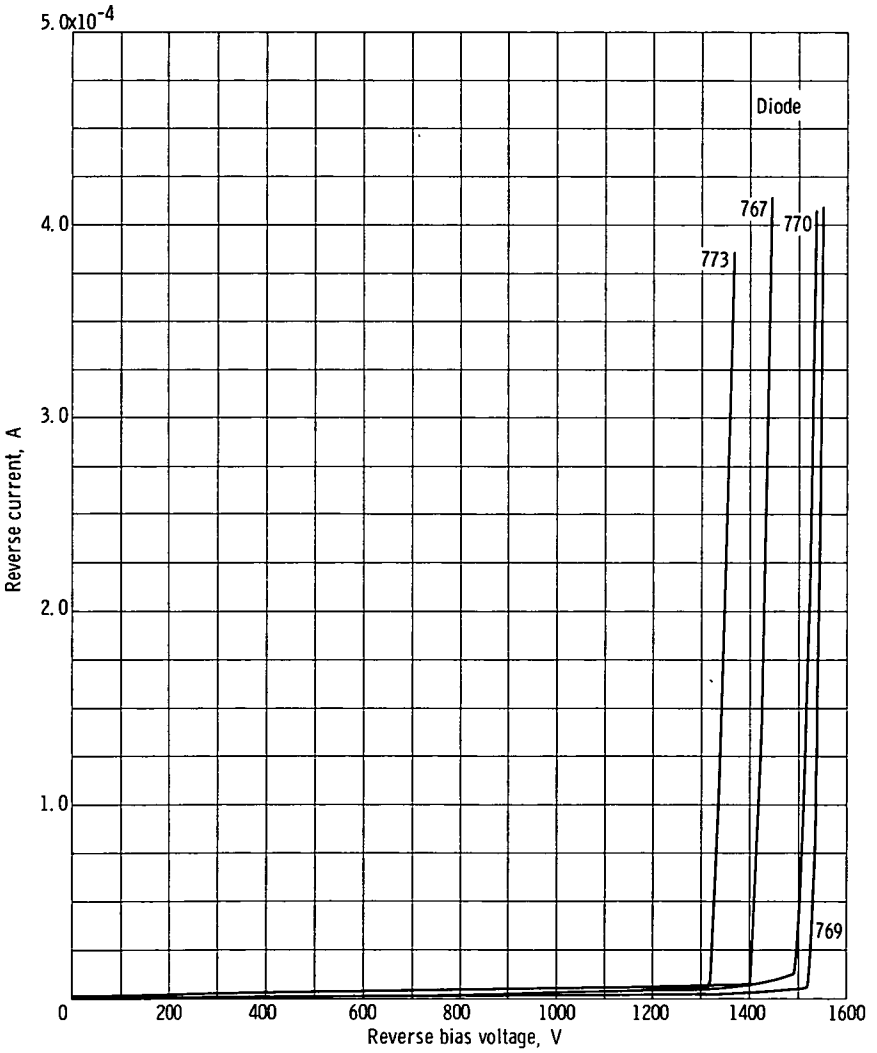

Figure 4. - X-Y plot of reverse current as a function of applied voltage including avalanche region for diodes 767, 769, 770, and 773 before irradiation.

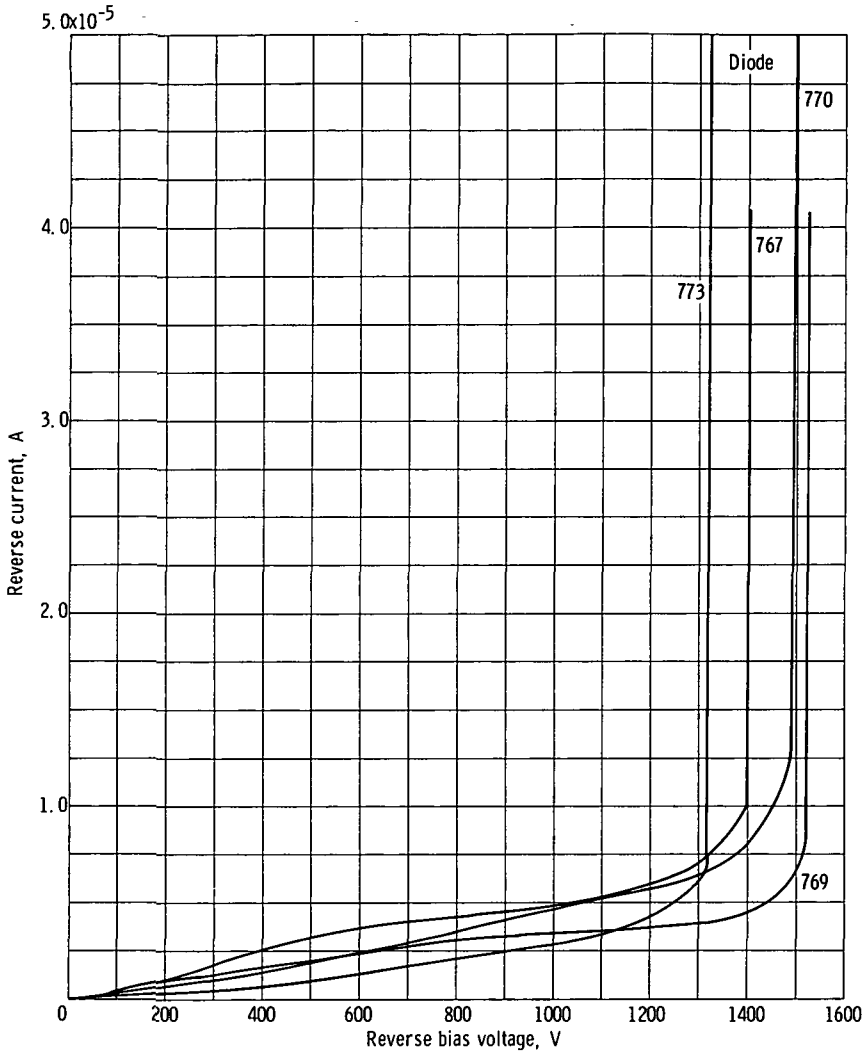

Figure 5. - X-Y plot of reverse current as a function of applied voltage including avalanche region for diodes 767, 769, 770, and 773 before irradiation. Expanded current axis.

voltage was increased, as one would expect from theory. The irregular curves were identified as those whose currents vary unevenly as the reverse voltage is increased. Both classes, however, had relatively sharp breakdown knees. Figures 4 and 5 are considered to be normal curves. Both figures are for the same group of diodes but figure 5 has the current axis expanded by a decade to 10^{-5} amperes. Figure 4 shows the higher breakdown voltages better while figure 5 shows the lower voltage-currents more clearly. It can be seen that in the expanded scales (fig. 5) diode 770 actually shows some irregularity in its characteristics whereas the rest have a relative smooth slope. Figures 6 and 7 are two sets of similar curves for the group of diodes considered to be irregular. Again figure 6 illustrates the higher voltage regions better than figure 7, whereas the curves of figure 7 show the lower voltage curve shapes better

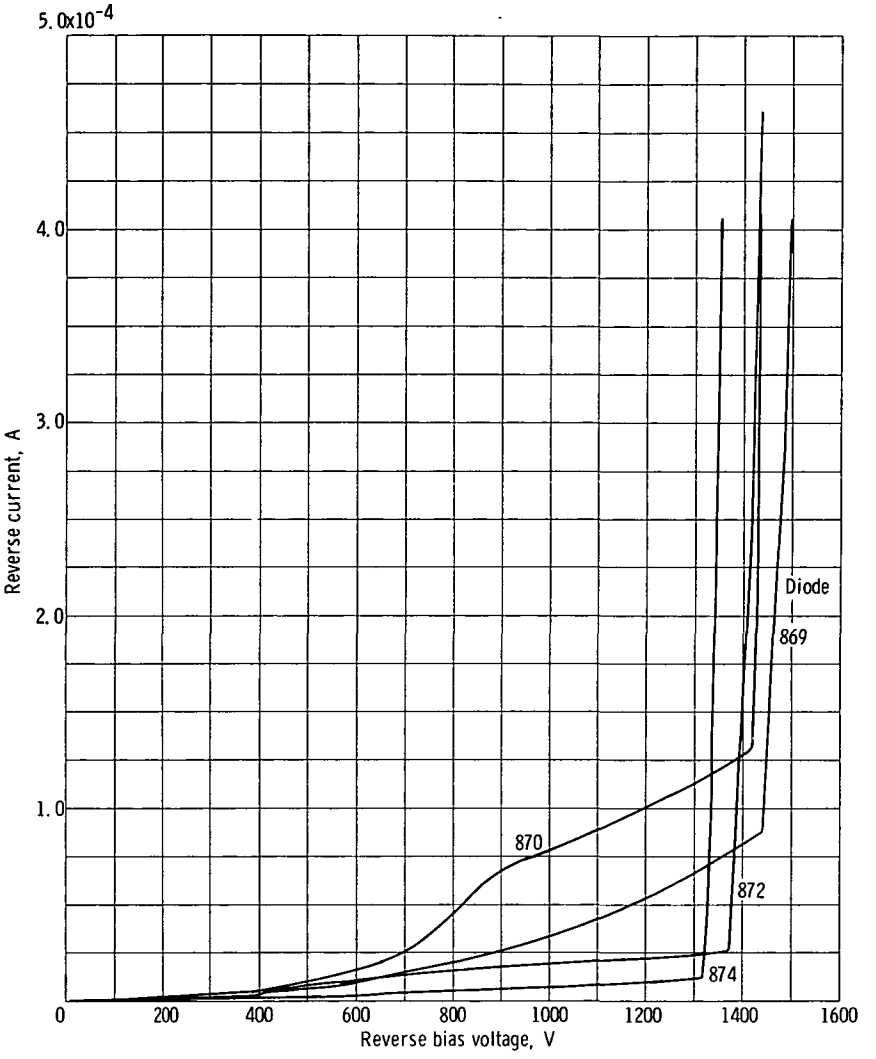

Figure 6. - X-Y plot of reverse current as a function of applied voltage including avalanche region for diodes 869, 870, 872, and 874 before irradiation.

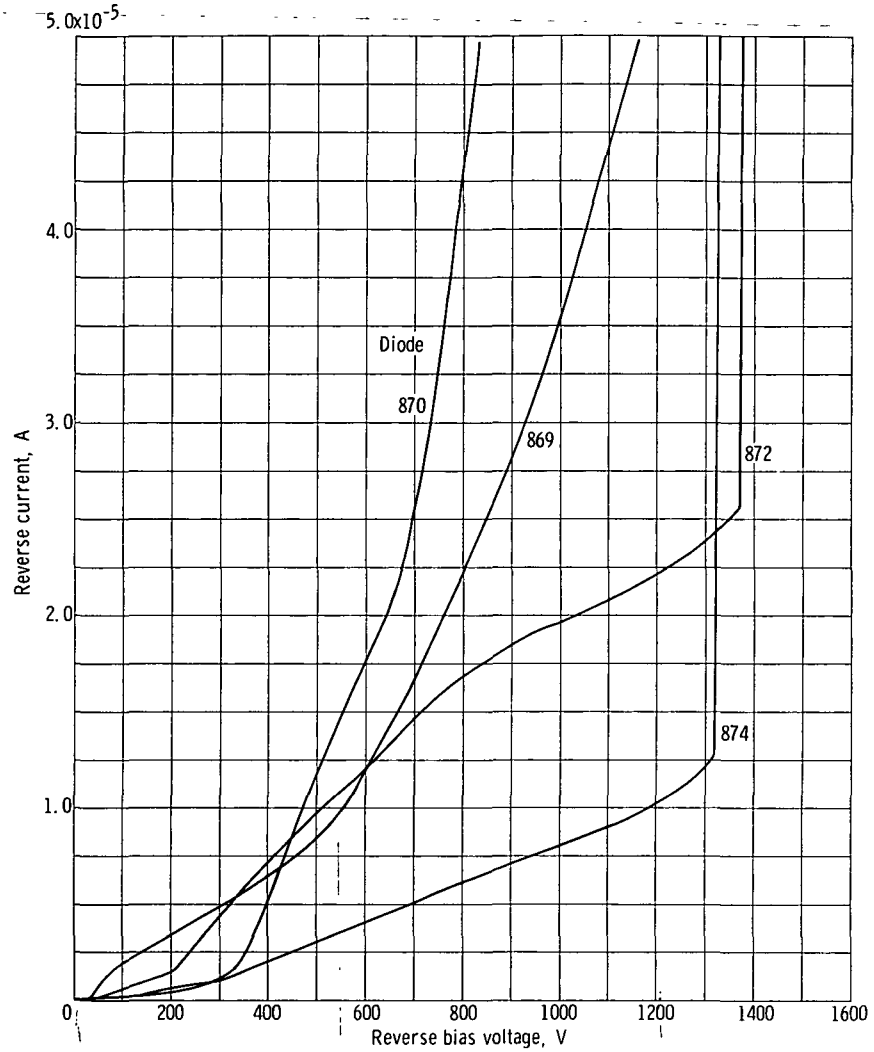

Figure 7. - X-Y plot of reverse current as a function of applied voltage including avalanche region for diodes 869, 870, 872, and 874 before irradiation. Expanded current axis.

than figure 6. In this group of diodes diode 874 could be considered nearly normal. These curves demonstrate the difficulty in classifying all curves as either normal or irregular and is at best a relative-type classification. These inconsistancies among the characteristics make a theoretical construction of curves to fit the experimental values in this voltage region virtually impossible. Also shown in figures 8 and 9 for test I and II, respectively, are the spreads in magnitudes of reverse currents for given voltages among all diodes tested. It can be seen the spread in reverse currents for 600 volts is over two decades with the averages for both tests approximately the same.

Others (ref. 11) have observed the irregular shapes of the reverse bias curves at higher voltages and have attributed this effect to uneveness of the junction. It is also possible that surface effects such as channeling may be involved but attempts to corre-

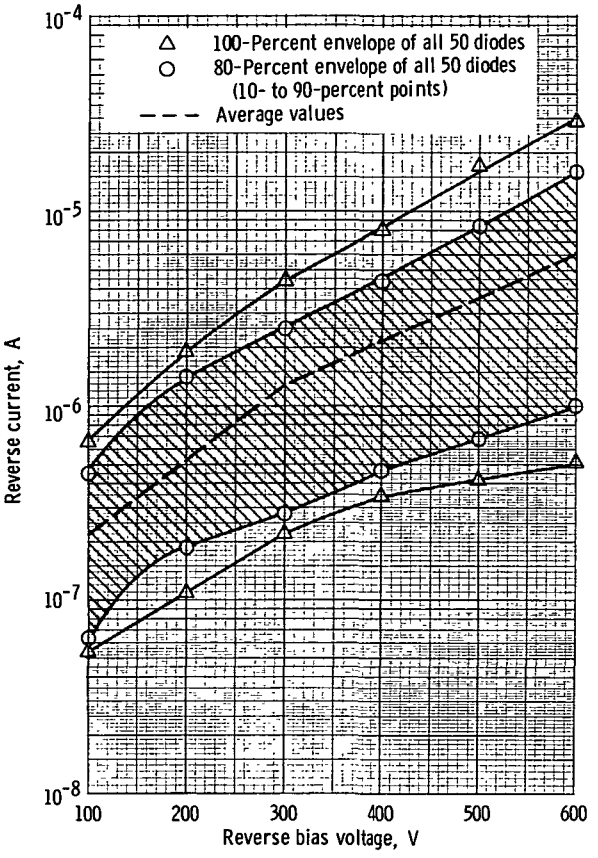

Figure 8. - Envelope of reverse currents as a function of reverse voltage for all diodes in test I before irradiation.

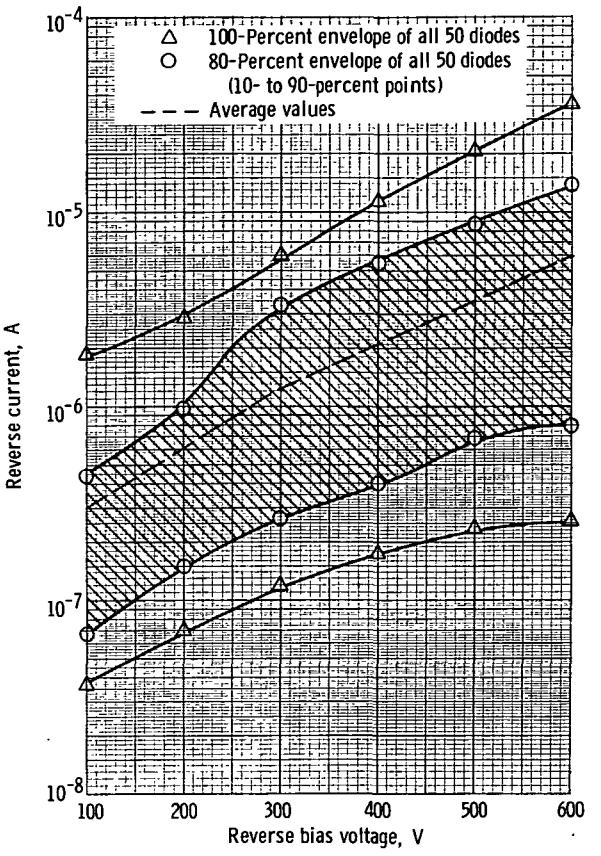

Figure 9. - Envelope of reverse currents as a function of reverse voltage for all diodes in test II before irradiation.

late calculated values of reverse current due to channeling and changes in capacitances of the junction, that possibly were due to channeling, were not successful. In fact, all electrical characteristics were examined in relation to each other to see if some of the irregularities in each could be correlated to the other but this was not successful.

Unlike the forward currents where the magnitude of the diffusion components of current is much larger than the surface component at higher bias regions, the reverse bias surface current, which was unpredictable in this test, can mask the generation-recombination and/or diffusion component at any reverse bias.

Effects of radiation damage at high reverse voltages. - The effects of radiation on the reverse currents at higher reverse voltages (100 V and above) are considerably less predictable than at the lower voltages. At these voltages, the magnitude of change in the reverse currents vary widely, and as in approximately 30 percent of the diodes the current decreases. These effects are demonstrated by diodes which were selected to illustrate the changes indicated, shown in figures 10 and 11. Again these two figures contain the same diodes but figure 11 has its current scale expanded so the current at lower voltages may be observed. Since this group of curves were considered to be

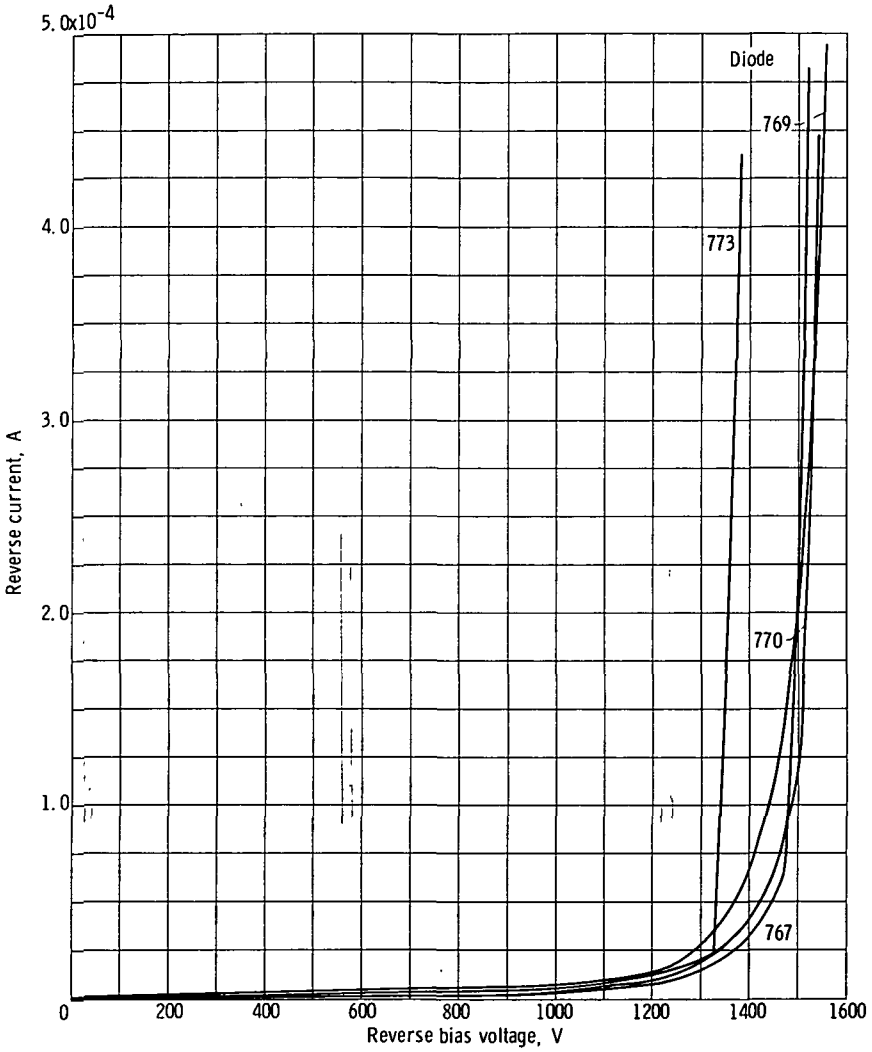

Figure 10. - X-Y plot of reverse current as a function of applied voltage including avalanche region for diodes 767, 769, 770, and 773 after neutron fluence of 4.4×10^{13} neutrons per square centimeter.

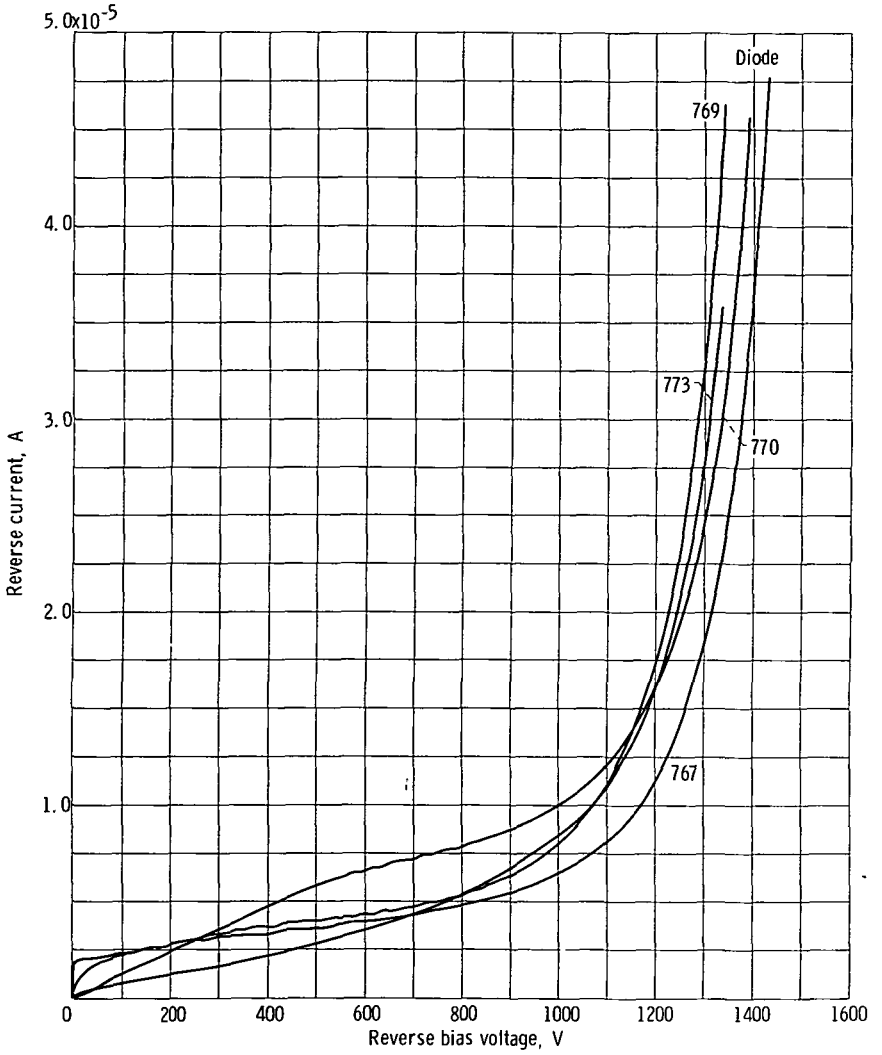

Figure 11. - X-Y plot of reverse current as a function of applied voltage including avalanche region for diodes 767, 769, 770, and 773 after neutron fluence of 4 4x10^{13} neutrons per square centimeter. Expanded current axis.

normal curves it can be seen by comparing the curves of the preirradiated diodes (figs. 4 and 5) that the currents increased with radiation as would be expected from generation-recombination theory. However, comparison of figures 12 and 13 with figures 6 and 7 show that for these diodes the currents actually decreased with radiation. This behavior appears typical of the irregularly shaped curves. Since there are many variations to the shapes of irregular curves, it is impossible to predict the magnitude of decrease in current for any given diode after irradiation. In some instances the irregular shape of a curve is almost entirely removed while in a few cases some irregular characteristics are taken on by normal curves after irradiation. Again attempts to correlate large changes in junction capacitance and forward voltage drops due to radiation

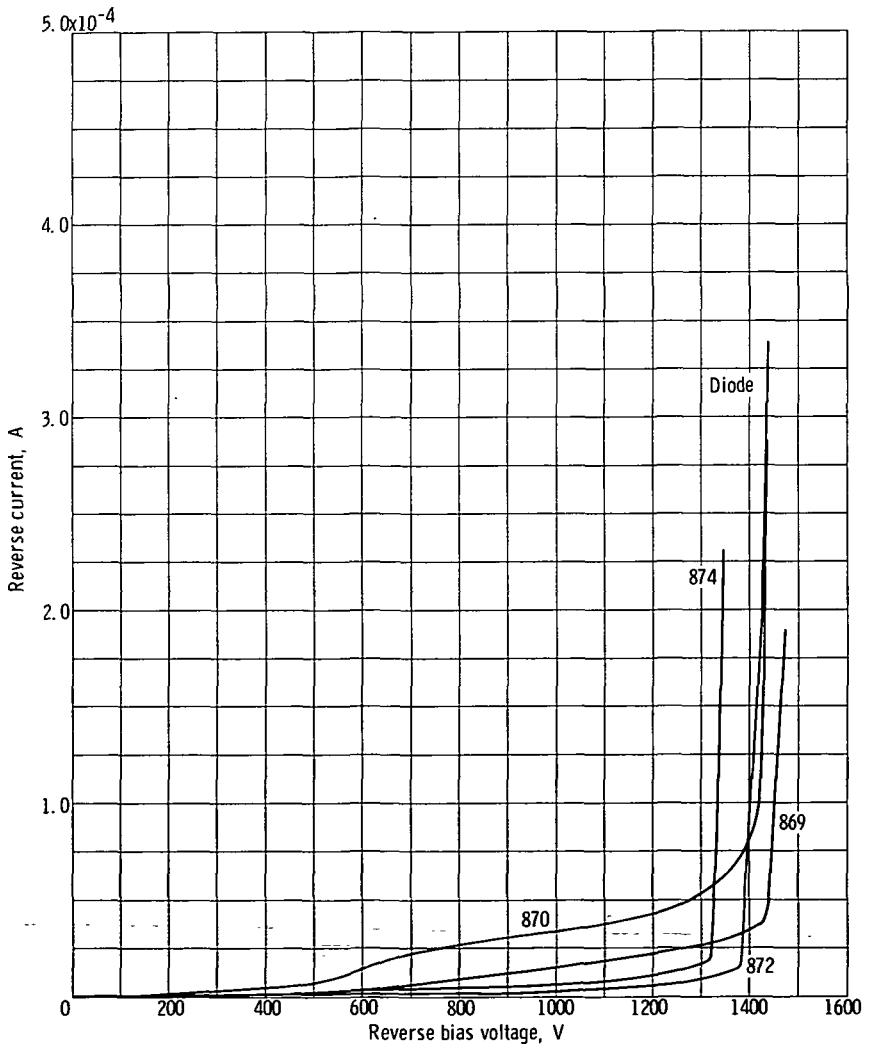

Figure 12. - X-Y plot of reverse current as a function of applied voltage including avalanche region for diodes 869, 870, 872, and 874 after neutron fluence of 4.7×10^{13} neutrons per square centimeter.

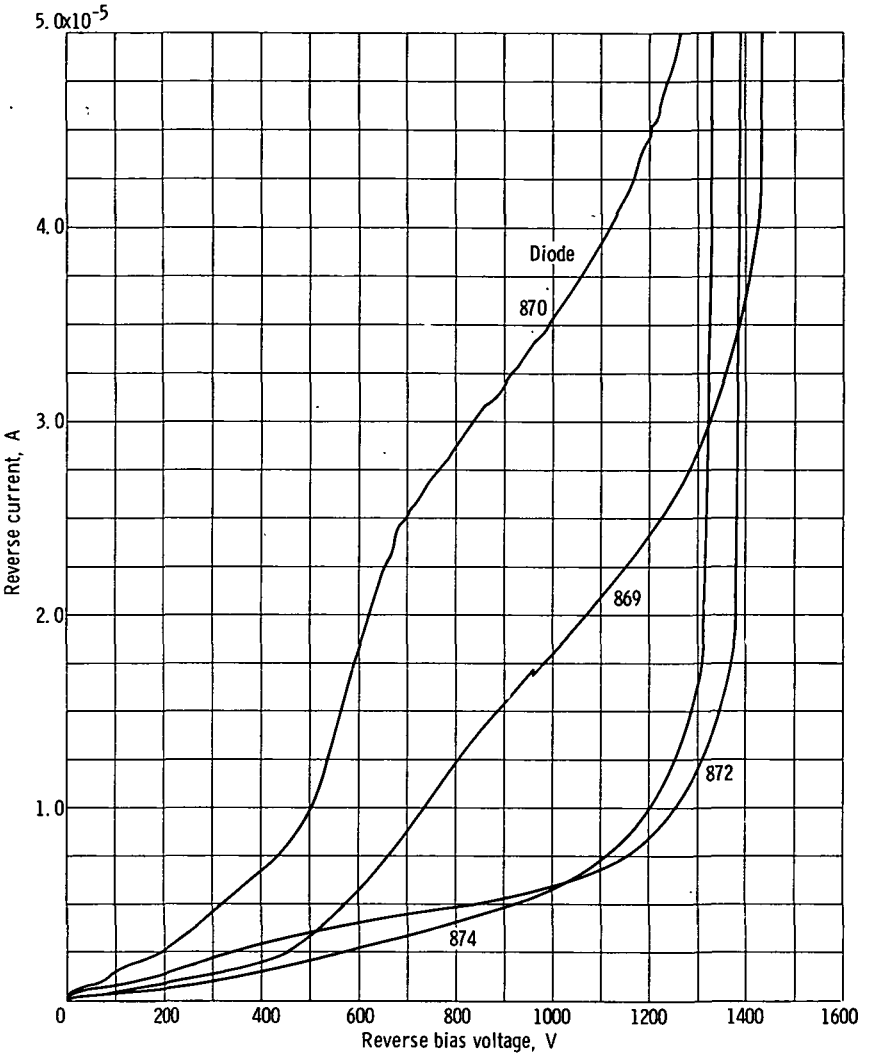

Figure 13. - X-Y plot of reverse current as a function of applied voltage including avalanche region for diodes 869, 870, 872, and 874 after neutron fluence of 4.7×10^{13} neutrons per square centimeter. Expanded current axis.

with the irregular curve shapes of reverse currents were not successful. It is not known at this time why irradiation affects the irregular curve shapes in the manner it does.

It was also of interest that out of 50 diodes in each test, one showed a much greater change in reverse current than the other forty-nine. This is shown in figures 14 and 15 for tests I and II, respectively. These curves also show the spread in values after irradiation. They show the 100 percent and 80 percent envelopes of the currents as well as the average values for each test and can be compared to the unirradiated curves in figures 8 and 9. It appears that, with the exception of the two diodes mentioned previously, the spread in values decreased in each test. This is understandable when consideration is given to the fact the lowest values increased more than the higher values of current

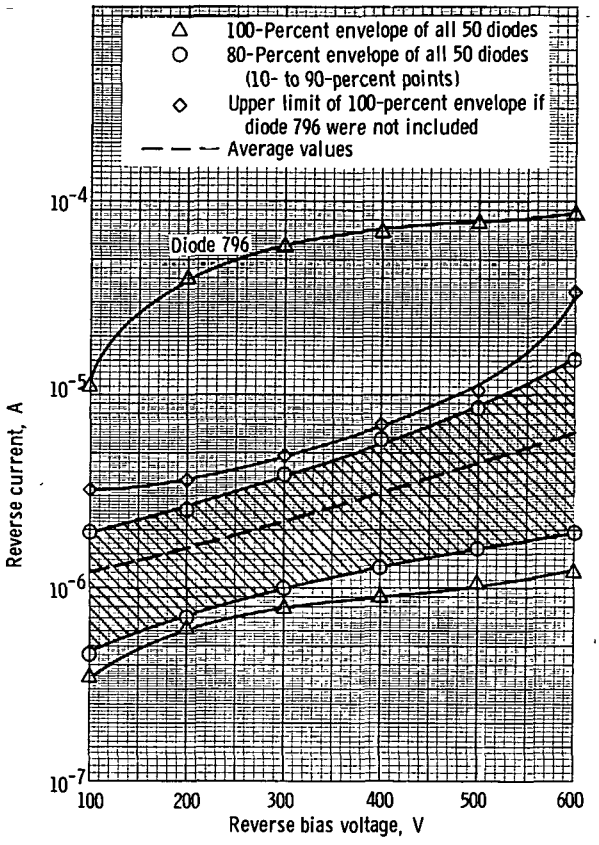

Figure 14. - Envelope of reverse currents as a function of reverse voltage for all diodes in test I after irradiation.

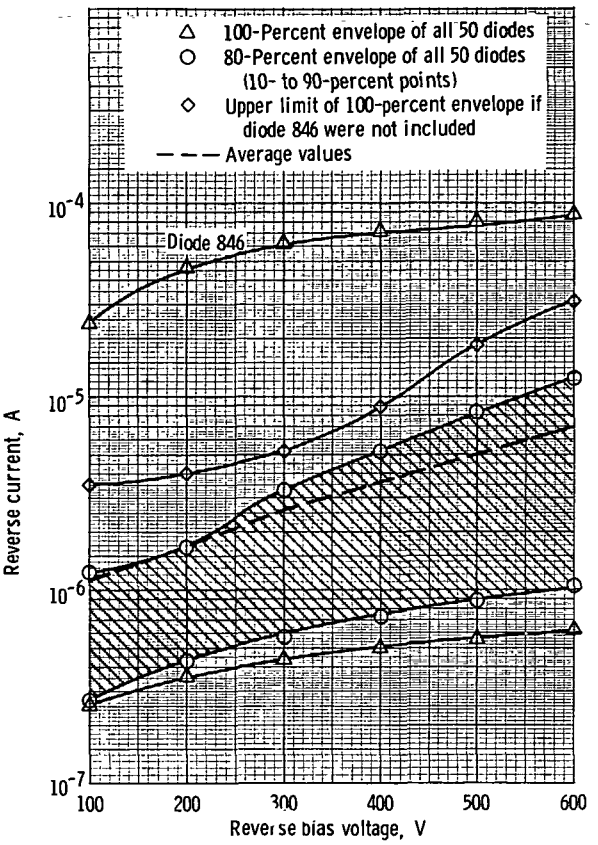

Figure 15. - Envelope of reverse currents as a function of reverse voltage for all diodes in test II after irradiation.

so in effect it would decrease the spread although the average value increased to a small extent. Also both the spread and average value would be affected by the fact that approximately 30 percent of the currents decreased with radiation.

Diodes 796 and 846 shown in figures 14 and 15, respectively, both had large increases in current and similar shaped curves after irradiation. An examination was made of their preirradiated curves to see if this would provide information that could be used to predict these large increases. Figure 16 shows the pre and postirradiated curves of diodes 796 and 846 as well as diodes 801 and 861 which had the lowest reverse currents of tests I and II, respectively, and diode 820, chosen because of its preirradiated similarity to diode 796. It can be seen that, although diode 820 had a higher reverse current before radiation, it changed very little with radiation, as compared to diode 796. The other curves only demonstrated the unpredictability of damage from the preirradiated curves.

Figures 17 and 18 show the increase in reverse currents at 100 volts reverse bias with increasing neutron fluence over two reactor cycles. Although there are breaks in the curves due to reactor shutdowns and scrams, the current shows a continued increase

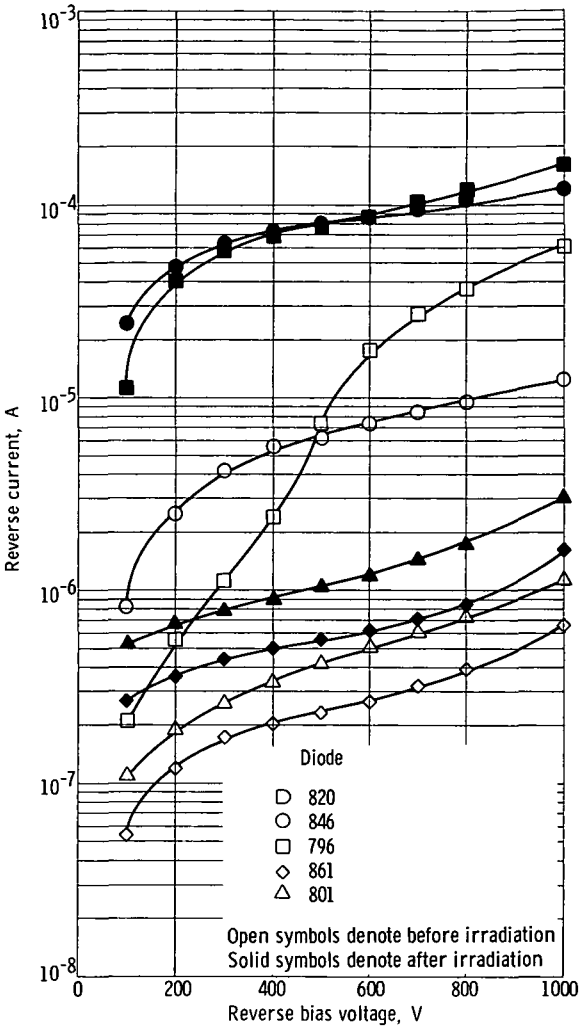

Figure 16. - Reverse currents as a function of reverse voltage of diodes displaying largest and smallest reverse currents.

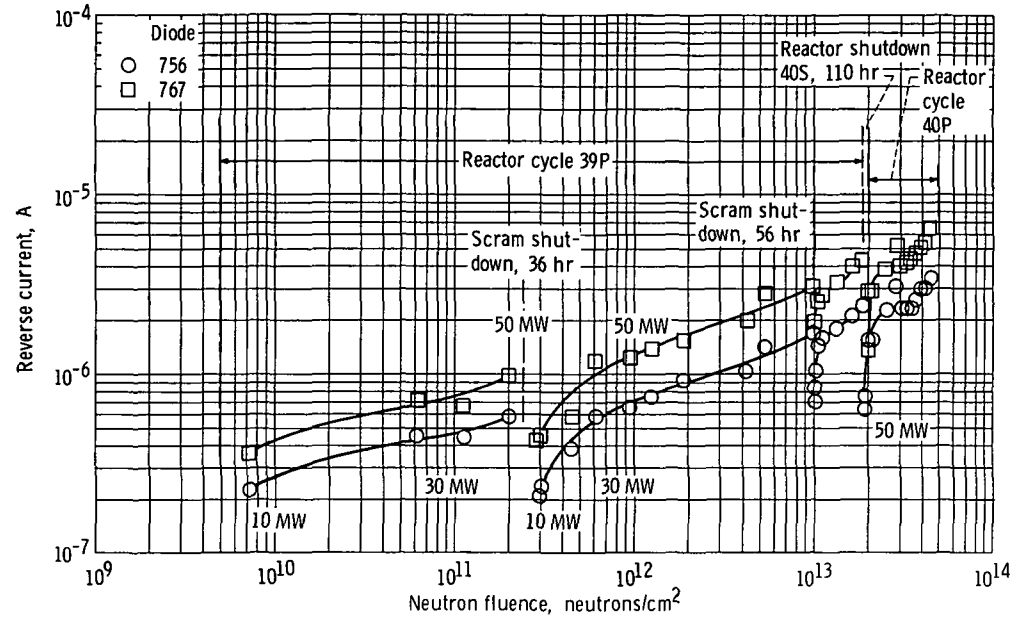

Figure 17. - Increase in reverse current at 100 volts reverse bias with neutron fluence for diodes 756 and 767. (All data taken at 60-MW reactor power unless indicated otherwise.)

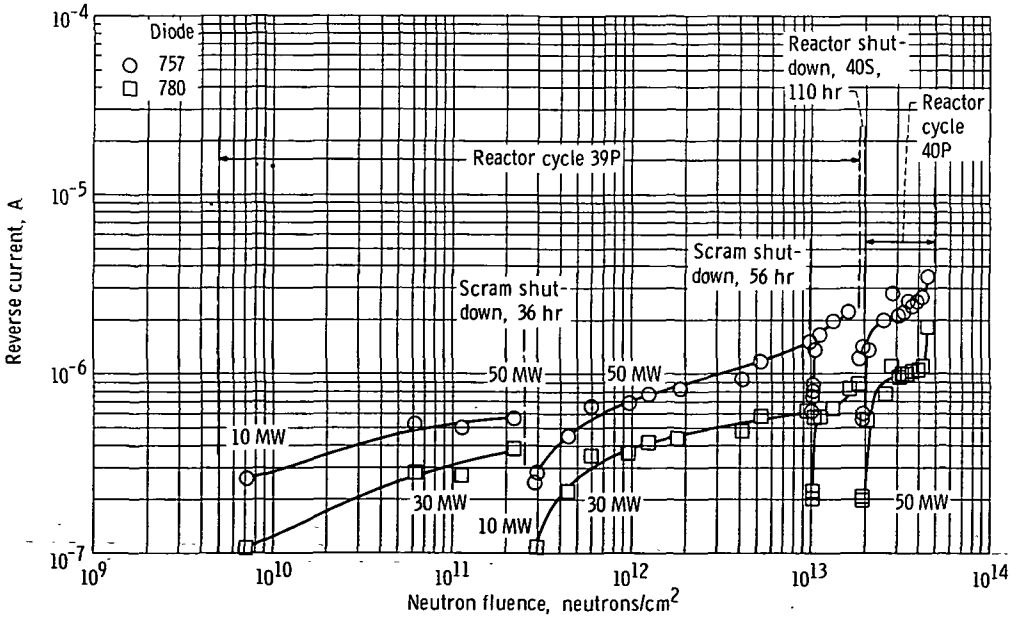

Figure 18. - Increase in reverse current at 100 volts reverse bias with neutron fluence for diodes 757 and 780. (All data taken at 60-MW reactor power unless indicated otherwise.)

over the two cycles. It is to be noted that data points were taken in several instances at different power levels of the reactor. This would not affect the increase in current due to neutron damage to the device; however, the small gamma ray photocurrents which are included in the readings would be affected by power levels. Figures 17 and 18 suggests also some annealing took place during the time that the reactor was shut down since it took considerable additional neutron fluence to recover to the same reverse currents.

To check the effects of annealing on the reverse currents, measurements were made on the diodes after the reactor was shut down but with the diodes still in the test cavity. The results are shown in figure 19. The initial sharp decrease in reverse current after reactor shutdown is probably due to the initial temperature drop of the test

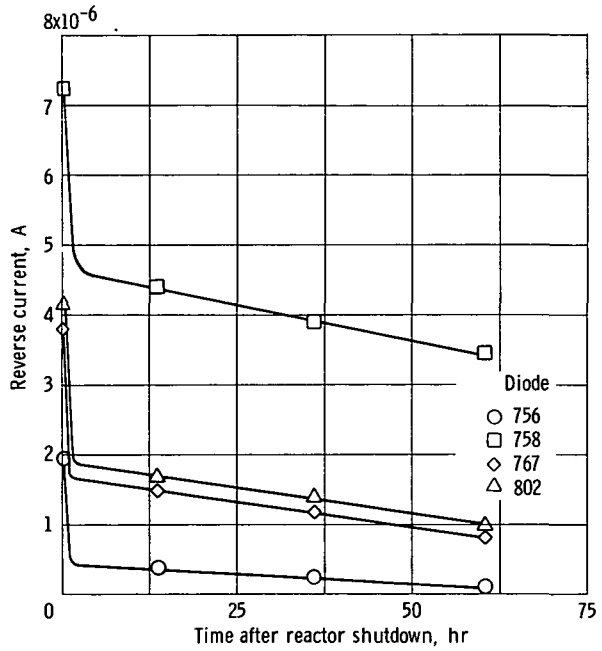

Figure 19. - Annealing curves showing change in reverse current with time after irradiation. Reverse bias voltage, 100 volts dc; reactor shutdown 40S.

facility. The gradual decrease out to 60 hours is most likely due to some type of room temperature annealing. The annealing appears to be insignificant in comparison to the changes due to radiation damage.

The diodes prior to irradiation have a very sharp voltage breakdown knee as shown in figure 20, which is considered as typical. They also have a relatively sharp voltage breakdown knee after irradiation, however, after irradiation there is a rounding or softening prior to the breakdown knee which would indicate greater multiplication in this

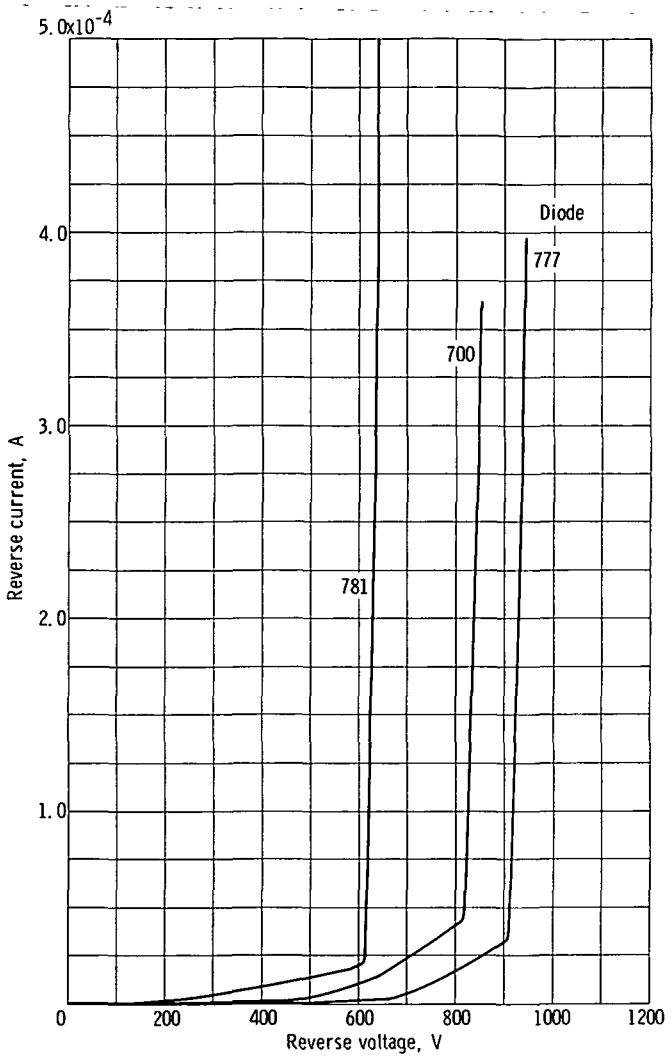

Figure 20. - X-Y plot of reverse current as a function of applied voltage for diodes 700, 777, and 781.

area than before irradiation.

Another equally obvious characteristic about the breakdown voltage for the 100 diodes is the spread in the breakdown voltage values. The values for breakdown voltages range from a little above 600 volts to as high as 1700 volts; and since the diodes are production-type models which are assumed similar in impurity levels, construction profiles, and dimensions, it is very difficult to isolate a particular parameter responsible for the variation. The diodes in figure 20 show a lower breakdown voltage than average for these diodes. A nominal value for voltage breakdown may be calculated using physical data on the chips furnished by the manufacturer. Using a linear grade approximation for the diffused junction with an exponential impurity distribution the grade constant can be expressed by (ref. 12)

$$a = \frac{N_a}{x_j} \ln \frac{N_o}{N_a}$$

where

N_a base impurity concentration of 1.4×10^{14} atoms/cm^3

N_o surface concentration of 10^{20} atoms/cm^3

x_j junction depth of 5.85×10^{-3} cm

Evaluating the previous equation results in

$$a = 3.22\times10^{17} \text{ (atoms)(cm}^{-4}\text{)}$$

Knowing the grade constant, the breakdown voltage can be calculated from an expression where the constants have been evaluated and lumped together (ref. 12)

$$V_{BR} = 1.7\times10^{9} \cdot a^{-0.364}$$

$$V_{BR} = 1.71\times10^{9}\left(3.22\times10^{17}\right)^{-0.364}$$

$$V_{BR} = 740 \text{ V}$$

Since the majority of the diodes have a larger breakdown voltage than this value, it is possible that the calculated grade constant is too high or that the values used for the geometry and concentration given by the manufacturer are in error.

Radiation Tolerance Improvement

There were two significant conclusions reached as a result of the testing, which affects the possibility of increasing the radiation tolerance of these diodes. These conclusions were that the reverse voltage breakdown in general did not change significantly with radiation at these neutron fluences and that although the reverse current increased it did not increase enough to limit the usefulness of the diode. It had been found previously (ref. 4) that the forward voltage drop at high injection levels would be the electrical characteristic which would limit the diodes use due to radiation. These three electrical characteristics have common controllable properties which can be optimized to increase the radiation tolerance of the forward voltage drop but at the expense of the

reverse current and breakdown voltages. These controllable parameters are the base thickness and base doping levels. Since the reverse breakdown voltages were in the general range of 1200 to 1500 volts, and the specified breakdown voltage was 600 volts, the breakdown voltage could be reduced considerably and yet remain within specifications. The reverse current in the 600-volt bias range were in the 10^{-7}- to 10^{-6}-ampere range even after irradiation. This suggests that by decreasing the base width and increasing the base doping the following could be accomplished:

(1) There would be a decrease in reverse breakdown voltage but it would not affect the useful lifetime because the breakdown voltage changes very little with radiation.

(2) A possible increase in surface leakage due to a shorter leakage path; however, there would be a lower generation-recombination bulk component due to the reduced volume of the depletion region.

(3) A decrease in forward voltage drop because of the increased conductivity across the base region and a smaller base thickness to diffusion length ratio (ref. 4). This would extend the useful lifetime of the diode in a nuclear environment.

CONCLUSIONS

The reverse bias electrical characteristics of 100 high reliability silicon power diodes were investigated with respect to the effects of nuclear radiation on these characteristics. The conclusions were as follows:

1. The preirradiated diodes had very low reverse currents and sharp avalanche voltage knees but there was considerable spread among the diodes in both reverse currents and breakdown voltages.

2. The postirradiated diodes had:

   a. Large percentage changes in reverse currents but not enough increase to limit the use of the diodes.

   b. Generally very little change in the breakdown voltages although there was considerable softening or rounding of the knee.

   c. No appreciable change in the amount of spread in the reverse characteristics.

3. The preirradiated reverse current curves generally fell into two classes:

   a. Normal curves where the current increased uniformly with increase in reverse bias. For these diodes the currents generally increased with radiation.

   b. Irregular curves whose reverse currents increase unevenly with increasing bias. The current generally decreases with radiation for these diodes. Approximately 30 percent of the diodes tested displayed this effect.

4. A theoretical curve was calculated along with an estimate of change in the reverse characteristics due to irradiation and compared to experimental values. Only fair

agreement was found at lower voltage up to approximately 100 volts. Calculations at higher voltages were not possible due to the irregular experimental curves.

5. The effects of irradiating the diodes at different temperatures and operating modes were not discernable due to the spread in experimental data.

6. Attempts to correlate the unusual changes such as decreases in currents with radiation with changes in junction capacitance and forward characteristics were unsuccessful.

7. The results of this test indicate how these diodes can be made more radiation tolerant by a trade-off of capabilities in the very low reverse currents and very high breakdown voltages for improved forward electrical characteristics.

Lewis Research Center,
National Aeronautics and Space Administration,
Cleveland, Ohio, June 25, 1973,
502-25.

APPENDIX A

SYMBOLS

A_j	area of junction, cm^2
a	grade constant
D_n	diffusion constant for electrons in silicon, cm^2/sec
I	reverse current, A
I_{ave}	reverse average current, A
I_D	diffusion current, A
I_{rg}	generation-recombination current, A
K	Boltzmann constant, eV/K
K_s	damage constant for silicon
L_n	low level diffusion length for electrons in p-region, cm
N_a	acceptor dopant concentration in p-region, cm^{-3}
N_u	surface concentration, $atoms/cm^3$
n_i	intrinsic carrier concentration, cm^{-3}
n_p	density of electrons in p-region under thermal equilibrium conditions, cm^{-3}
q	charge on electron, C
T	temperature, K
V_A	applied voltage, V
V_B	built-in voltage at junction (diffusion potential), V
V_{BR}	reverse breakdown voltage, V
W	depletion region width, cm
x_j	junction depth, cm
φ	neutron fluence, $neutrons/cm^2$
τ_{eff}	effective minority carrier life time, sec
τ_{no}	limiting lifetime for electrons in heavily doped p-region, sec
τ_{po}	limiting lifetime for holes in heavily doped n-region, sec

APPENDIX B

REVERSE CURRENT CALCULATIONS

The reverse applied voltages in the few tenths of a volt range are of little importance generally as far as circuit application is concerned since the values of current are so small. The current-voltage data in this region does, however, furnish useful information as to the validity of the analytical approach and the physical parameters used in the calculations.

As in the forward bias diodes, the reverse currents are made up of three components, generation-recombination, diffusion, and surface. Unlike the forward current, however, as the reverse bias is increased the diffusion component becomes a small factor while the generation-recombination becomes the dominant component. The surface component is less predictable but undoubtedly contributes at all values of reverse bias. The diffusion and generation-recombination components are calculable and can be added for comparison with experimental values.

The generation-recombination component of the reverse current is due to the net generation-recombination of carriers in the depletion region of the n^+-p and p-p^+ junctions (regions 2 and 4, respectively, of fig. 21). The current contributed by the p-p^+

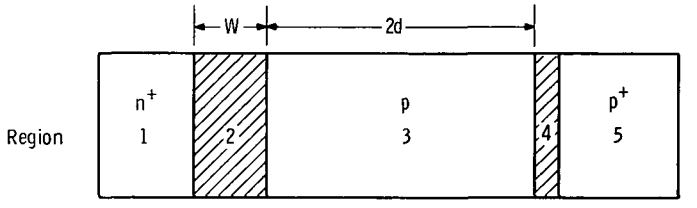

Figure 21. - Different dopant and depletion regions of n^+-p-p^+ silicon chip.

depletion region is small compared to that of the n^+-p so that only that component due to region 2 need be considered. The equation for the generation-recombination current I_{rg} was developed by Sah, Noyce, and Shockley (ref. 1) where the net generation-recombination rate expression was integrated over the depletion region width; it is

$$I_{rg} = \frac{2qn_i WA_j \sinh \frac{qV_A}{2KT}}{\sqrt{\tau_{po}\tau_{no}}\,(V_B - V_A)\frac{q}{KT}} f(b) \qquad \text{(B1)}$$

Reverse I_{rg} was calculated using the following values for the physical parameters:

Parameter	Value	Source
Area of junction, A_j, cm^2	0.455	Obtained from manufacturer
Intrinsic carrier concentration, n_i, carriers/cm^3	1.5×10^{10}	Ref. 12
Depletion region width[a], W, cm	4.5×10^{-4}	Value for zero bias obtained from junction capacitance measurements
$\sqrt{\tau_{po}\tau_{no}}$, sec	[b] 5×10^{-6}	Obtained from manufacturer
Built-in voltage at junction, V_B, V	0.35	Obtained from junction capacitance-voltage measurements
KT/q (at 300 K), V	0.026	Calculated
f(b)[c]	0.05	Ref. 1

[a] At zero and very low reverse bias; increases proportional to $(V - V_{1/3})$ at low reverse bias changing to $V^{1/2}$ at larger reverse bias (ref. 13).

[b] An effective minority carrier lifetime.

[c] For low applied bias only.

The expression for f(b) is

$$f(b) = \frac{1}{2\sqrt{b^2 - 1}} \ln \frac{b + \sqrt{b^2 - 1}}{b\sqrt{b^2 - 1}} \quad \text{for } b > 1$$

where

$$b = e^{-qV_A/KT}\left(\cosh\frac{E_t - E_i}{KT} + \ln\sqrt{\frac{\tau_{po}}{\tau_{no}}}\right)$$

The $\left[\cosh (E_t - E_i/KT) + \ln \sqrt{\tau_{po}/\tau_{no}}\right]$ term was calculated to be 108.5, where $E_t - E_i = 0.14$ eV was evaluated from the slope of the reverse current divided by $T^{3/2}$ against reciprocal temperature curve in figure 22 (ref. 1) at 5.0 volts bias. Also τ_{po} was assumed to be equal to τ_{no}.

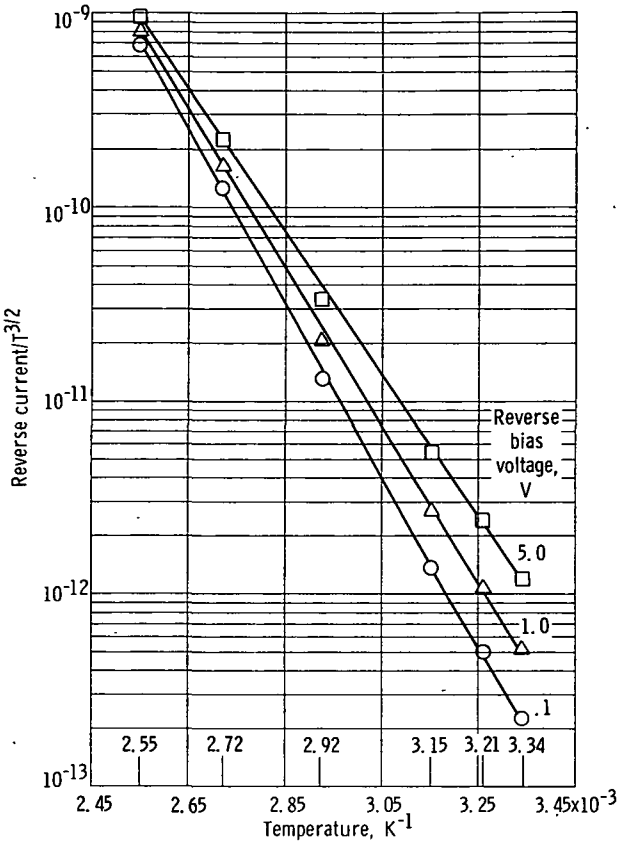

Figure 22. - Reverse current as a function of reciprocal of temperature for diode 819 before irradiation.

The diffusion component of the reverse current makes a significant contribution up to approximately 0.10 volt. Above this value it is essentially constant so it becomes less significant as the reverse bias is increased. The diffusion component is summed with the generation-recombination component for comparison with the experimental values. The diffusion current expression used for this computation is (refs. 12 and 13) the following:

$$I_D = \left(\frac{qAD_n n_p}{L_n}\right)\left(e^{qV_A/KT} - 1\right) \tag{B2}$$

and is applicable to this type diode where the n^+m region is much more heavily doped than the p-base region.

The following values for the various parameters were used in the calculations:

Parameter	Value	Source
Temperature, T, K	300	----------
Density of electrons in p-region under thermal equilibrium conditions, n_p, electrons/m^3	1.6×10^{6}	Calculated from base doping $n_p = \frac{(n_i)^2}{N_a}$
Diffusion constant for electrons in silicon, D_n, cm^2/sec	30	Ref. 12
Low level diffusion length for electrons in p-region, L_n, cm	1.22×10^{-2}	Calculated from minority carrier lifetime $L_n = \sqrt{D_n \tau_n}$

The resistive component of current was calculated from Ohm's law relation where the surface resistance was assumed to be 10^9 ohms.

APPENDIX C

CALCULATION OF A SILICON DAMAGE CONSTANT

One way to observe the neutron damage effects in the diodes is to calculate a damage constant. Data taken during irradiation for reverse currents for nine diodes were used to calculate a damage constant following the methods of others in the field (refs. 3 and 9). If the equation relating generation current to lifetime is expressed as

$$I_{rg} = \frac{qn_i AW}{\tau} \tag{C1}$$

and the degradation of the minority lifetime τ with radiation is expressed as

$$\frac{1}{\tau} = \frac{1}{\tau_o} + K_s \varphi \tag{C2}$$

where

τ postirradiated minority carrier lifetime

τ_o preirradiated minority carrier lifetime

K_s damage constant for silicon

φ neutron fluence

Substituting $1/\tau$ into equation (C1) for the generation current results in

$$I_{rg} = \frac{qn_i AW}{\tau_o} + qn_i AWK_s \varphi$$

If I_{rg_o} represents the generation current before irradiation, then

$$I_{rg_o} = \frac{qn_i AW}{\tau_o}$$

so that $\Delta I_{rg} = I_{rg} - I_{rg_o} = qn_i AWK_s \varphi$ and

$$K_s = \frac{1}{qn_iAW} \frac{\Delta I_{rg}}{\varphi} \qquad (C3)$$

Data from the first reactor cycles of tests I and II were used in determining the damage constant K_s for silicon. These corresponded to cycles designated 39P and 41P, respectively. The neutron fluence used was chosen from a portion of each cycle which represented the least interruption of the flux due to shutdowns, start up or changing power levels. Selections were based also on the fact that these particular cycles had a minimum of interruptions and the diodes had been exposed to a minimum of neutron flux oscillations unlike the later cycles 40P and 42P. The change in reverse current with flux varies considerably among the diodes so that the calculated damage constants also have considerable variations. Due to this variation, the average change in reverse current of nine diodes was used in the calculations for the damage constant for each test. The reverse currents were taken at 100 volts reverse bias and although the operating temperature for cycle 41P was 125° C, the measurements were taken when the diodes temperatures were stabilized at around 28° C.

Values for K_s were calculated using the following:

$$q = 1.6\times10^{-19}$$

$$n_i = 1.5\times10^{10}$$

$$A = 0.455 \text{ cm}^2$$

$$W = 4.0\times10^{-3} \text{ cm}$$

$$\varphi = 1.0\times10^{13} \text{ neutrons/cm}^2 \text{ (cycle 39P)}$$

$$\varphi = 1.34\times10^{13} \text{ neutrons/cm}^2 \text{ (cycle 41P)}$$

$$\Delta I_{ave} = 1.6\times10^{-6} \text{ A (cycle 39P)}$$

$$\Delta I_{ave} = 0.95\times10^{-6} \text{ A (cycle 41P)}$$

The values for K_s were 3.6×10^{-8} cm^2 neutron^{-1} sec^{-1} for cycle 39P and 1.6×10^{-8} cm^2 neutron^{-1} sec^{-1} for cycle 41P. These values are in general agreement with damage constants found by others (ref. 3). However, the damage constant for cycle 41P could be lower due to the annealing effects of the higher operating temperatures during that cycle. Using these damage constants and the preirradiated lifetimes for the minority

carriers, the postirradiated lifetime may be calculated using equation (C2). These lifetimes are 5.4×10^{-7} and 1.0×10^{-6} second for cycles 39P and 41P, respectively.

REFERENCES

1. Sah, Chih-Tang; Noyce, Robert N.; and Shockley, William: Carrier Generation and Recombination in P-N Junctions and P-N Junction Characteristics. Proc. IRE, vol. 45, no. 9, Sept. 1957, pp. 1228-1243.

2. Sah, Chih-Tang: Effects of Electrons and Holes on the Transition Layer Characteristics of Linearly Graded P-N Junctions. Proc. IRE, vol. 49, no. 3, Mar. 1961, pp. 613-618.

3. Larin, Frank: Radiation Effects in Semiconductor Devices. John Wiley & Sons, Inc., 1968.

4. Been, Julian F.: Effects of Nuclear Radiation on a High-Reliability Silicon Power Diode. II - Analysis of Forward Electrical Characteristics. NASA TN D-5732, 1970.

5. Anon.: Screening Specifications for Semiconductor Device SIN1189. NASA Marshall Space Flight Center, Apr. 1963.

6. Davies, R. L.; and Gentry, F. E.: Control of Electric Field at the Surface of P-N Junctions. IEEE Trans. of Electron Devices, vol. ED-11, no. 7, July 1964, pp. 313-323.

7. Bozek, John M.; and Godlewski, Michael P.: Experimental Determination of Neutron Fluxes in Plum Brook Reactor HB-6 Facility with Use of Sulfur Pellets and Gold Foils. NASA TM X-1497, 1968.

8. Bozek, John M.: Experimental Determination of Gamma Exposure Rate in Plum Brook HB-6 Facility. NASA TM X-1490, 1968.

9. Frank, Max; and Taulbee, Carl D.: Handbook for Predicting Semiconductor Device Performance in Neutron Radiation. Bendix Corp., Mar. 1967. (Contract AF29(601)-7110).

10. Messenger, George C.; et al.: Device Performance Characteristics as Related to Radiation Damage in Semiconductor Materials. Rep. ARD-66-42-R, Northrop Corp. (AFCRL-66-462, DDC No. AD-643703), June 1966.

11. Batdorf, R. L.; Chynoweth, A. G.; Dacey, G. C.; and Foy, P. W.: Uniform Silicon P-N Junctions. I. Broad Area Breakdown. J. Appl. Phys., vol. 31, no. 7, July 1960, pp. 1153-1160.

12. Phillips, Alvin B.: Transistor Engineering and Introduction to Integrated Semiconductor Circuits. McGraw-Hill Book Co., Inc., 1962.

13. Lindmayer, Joseph; and Wrigley, Charles Y.: Fundamentals of Semiconductor Devices. D. Van Nostrand Co., Inc., 1965.

NATIONAL AERONAUTICS AND SPACE ADMINISTRATION
WASHINGTON, D.C. 20546

OFFICIAL BUSINESS
PENALTY FOR PRIVATE USE $300

SPECIAL FOURTH-CLASS RATE
BOOK

POSTAGE AND FEES PAID
NATIONAL AERONAUTICS AND
SPACE ADMINISTRATION
451

U.S.MAIL

POSTMASTER : If Undeliverable (Section 158 Postal Manual) Do Not Return

"The aeronautical and space activities of the United States shall be conducted so as to contribute . . . to the expansion of human knowledge of phenomena in the atmosphere and space. The Administration shall provide for the widest practicable and appropriate dissemination of information concerning its activities and the results thereof."

—NATIONAL AERONAUTICS AND SPACE ACT OF 1958

NASA SCIENTIFIC AND TECHNICAL PUBLICATIONS

TECHNICAL REPORTS: Scientific and technical information considered important, complete, and a lasting contribution to existing knowledge.

TECHNICAL NOTES: Information less broad in scope but nevertheless of importance as a contribution to existing knowledge.

TECHNICAL MEMORANDUMS: Information receiving limited distribution because of preliminary data, security classification, or other reasons. Also includes conference proceedings with either limited or unlimited distribution.

CONTRACTOR REPORTS: Scientific and technical information generated under a NASA contract or grant and considered an important contribution to existing knowledge.

TECHNICAL TRANSLATIONS: Information published in a foreign language considered to merit NASA distribution in English.

SPECIAL PUBLICATIONS: Information derived from or of value to NASA activities. Publications include final reports of major projects, monographs, data compilations, handbooks, sourcebooks, and special bibliographies.

TECHNOLOGY UTILIZATION PUBLICATIONS: Information on technology used by NASA that may be of particular interest in commercial and other non-aerospace applications. Publications include Tech Briefs, Technology Utilization Reports and Technology Surveys.

Details on the availability of these publications may be obtained from:

SCIENTIFIC AND TECHNICAL INFORMATION OFFICE

NATIONAL AERONAUTICS AND SPACE ADMINISTRATION

Washington, D.C. 20546